Electronic Supplementary Material (ESI) for ChemComm.

In situ visualization of peroxisomal peroxynitrite in liver of mice with acute liver injury induced by carbon tetrachloride using a new two-photon fluorescence probe

Yongqing Zhou,‡[a] Ping Li,‡[a] Nannan Fan,[a] Xin Wang,[a] Xiaoning Liu, [a] Lijie Wu,[a] Wen Zhang,[a] Wei Zhang,[a] Changle Ma,*[b] and Bo Tang*[a]

[a.] *College of Chemistry, Chemical Engineering and Materials Science, Key Laboratory of Molecular and Nano Probes, Ministry of Education, Collaborative Innovation Center of Functionalized Probes for Chemical Imaging in Universities of Shandong, Shandong Normal University, Jinan 250014, People's Republic of China.*

[b.] *College of Life Sciences, Shandong Normal University, Jinan 250014, PR China*

E-mail: tangb@sdnu.edu.cn changlema@yahoo.com

Table of Contents

Materials and Instruments

All reagents and solvents were purchased from commercial suppliers and used with not further purification. 3-(4,5-Dimethylthiazol-2-yl)-2,5-diphenyl tetrazolium bromide (MTT) was purchased from Sigma. 3-Morpholino sydnonimine hydrochloride (SIN-1), which generates both superoxide anion and nitric oxide that spontaneously form peroxynitrite ($ONOO^-$), was purchased from Sigma Chemical Company. Peroxisome-GFP was purchased from Invitrogen (U.S.A.). Silica gel (200−300 mesh) used for flash column chromatography was purchased from Qingdao Haiyang Chemical Co., Ltd. ^1H NMR and ^{13}C NMR spectra were determined at 400 MHz and 100 MHz using Bruker NMR spectrometers. The mass spectra were obtained by a Bruker Maxis ultrahigh-resolution time-of-flight mass spectrometry (TOF MS) system and the LCQ fleet ion trap mass spectrometer (Thermo Scientific, San Jose, CA, U.S.A.). The MTT assay was performed using a TRITURUS microplate reader. Absorption spectra were recorded on a UV-Vis spectrophotometer (Evolution 220, Thermo Scientific). The fluorescence spectrum measurements were performed using a Hitachi F-4600 fluorescence spectrophotometer (Japan, HITACHI). Confocal fluorescence imaging in cells and in mice was performed with a Zeiss LSM 880 NLO (two-photon) confocal laser scanning microscope. The co-localized images were recorded on a Leica TCS SP8 microscope with a 63x oil-immersion objective (N/A 1.3). The hepatoma cells (SMCC-7721) and liver cells HL-7702 cells were purchased from the Cell Bank of the Chinese Academy of Sciences (Shanghai, China). Peroxynitrite ($ONOO^-$) was chemically prepared by H_2O_2 and $NaNO_2$, the concentration of it was estimated by using an extinction coefficient of 1670 M^{-1} cm^{-1} (302 nm); $O_2^{\bullet-}$ was prepared by dissolving KO_2 in DMSO solution. Hydroxyl radical (•OH) was produced by the Fenton reaction (Fe^{2+}: H_2O_2 = 1: 10). NO was prepared from sodium nitroprusside. Hydrogen peroxide (H_2O_2), sodium hypochlorite (NaClO) and tert-butyl hydroperoxide (TBHP) were derived from water solutions with contents of 30 %, 10 % and 70 %, respectively. Solutions of metal ions were prepared from chlorizated salts, which were dissolved in deionized water.

Cell culture

HL-7702 and SMMC-7721 cells were cultured in DMEM and RPMI 1640 medium, respectively, supplemented with 10 % fetal bovine serum (Invitrogen), 1 % penicillin, and 1 % streptomycin. The cells were seeded in confocal culture dishes and then incubated for 24 h at 37 °C under a humidified atmosphere containing 5 % CO_2.

Cell imaging

The cells were detached and replanted on glass-bottomed dishes Before SMMC-7721 cells imaging. For monitoring of endogenous $ONOO^-$ in SMMC-7721 cells, cells were exposed to SIN-1 (1.0 mM, 30 min); then, they were treated with PX-1 (5 μM, 30 min) before being washed three times with PBS. For the scavenging assay, cells were treated with uric acid (100 μM, 2 h) in advance, followed by incubation with PX-1 (5 μM, 30 min). Two-photon fluorescence imaging was performed on a Zeiss LSM 880 confocal microscope upon excitation at 800 nm. To study PX-1 specically targeted peroxisome, cells also were exposed to SIN-1 (1.0 mM, 30 min); then, they were treated with PX-1 (5 μM), Peroxisome-GFP and others organelles before being washed three times with PBS. The time-dependent fluorescence imaging of SMMC-7721 cells incubated with PX-1. SMMC-7721 cells incubated with SIN-1 (1.0 mM) for 30 min, then treated with PX-1 (5.0 μM) and Mito-Tracker Deep Red (100 nM) for 15 min. The SMMC-7721 cells have good intact shape before they are imaged. The cells Co-images and time dependent fluorescence

images were recorded on a Leica TCS SP8 microscope with a 63x oil-immersion objective (N/A 1.3).

Mouse models and in vivo liver imaging

The C57 mice (female, 5-7 weeks old, 15-20 g) were purchased from the laboratory animal center of Shandong University (Jinan, China). All animal experiments were conducted at the laboratory of Shandong Normal University in compliance with the Guidelines of Shandong Normal University for the Care and Use of Laboratory Animals.

For monitoring in vivo livers $ONOO^-$ during CCl_4 induced acute liver injury. C57 mice were randomly divided into three groups, control group, experimental group and scavenger group. For the experimental group and scavenging group, the mice were treated with the same dose carbon tetrachloride (CCl_4, 2.4 $g \cdot kg^{-1}$) by intragastric administration for 48 h. Scavenging group was intraperitoneally treated uric acid (300 $mg \cdot kg^{-1}$) for another 2 h. The control group were treated with the same concentration saline by intragastric administration. The mice were performed a surgery operation to expose the liver for two-photon imaging after were intravenously injected with PX-1 (100 μL, 10^{-4} M) for 30 min. The C57 mice were fasted for 12 h to avoid possible food fluorescence interference to the dye fluorescence before imaging.

Statistical analysis

The data were accumulated from at least three independent experiments in same condition. All data are expressed as the mean ± S.D. For each experiment, unless otherwise noted, n represents the number of individual biological replicates. The statistical analyses were performed using Student's t-test. $P < 0.05$ was considered statistically significant.

For cell imaging, we first randomly selected three images. Then, we selected the three ROIs in one image to calculate average fluorescence intensity. To normalize the fluorescence intensity of images, the average fluorescence intensity of the control group referenced as "1". The fluorescence intensity of other groups were compared with the control group to obtain relative fluorescence intensity of (b) and (c) in Fig.2 of revised manuscript.

For in vivo imaging, we first collected the average fluorescence intensity of the whole spectrum in three experiments. Then, to normalize the fluorescence intensity of images, the average fluorescence intensity of the control group referenced as "1". The fluorescence intensity of other groups were compared with the control group to obtain relative fluorescence intensity experimental group and scavenger group. The results are shown in Fig.4 of revised manuscript.

Fluorescence quantum yield and measurement of the two-photon absorption cross-section.

(a) Fluorescence quantum yield

We choose fluorescein, which has a fluorescence quantum yield of 0.95 in ethanol, as the reference. According to the following standard equation (1), the quantum yield of PX-1 and PX-OH were determined to be 0.004 and 0.151, respectively.

$$\varphi_1 = \frac{\varphi_B I_1 A_B \lambda_{exB} \eta_1}{I_B \ A_1 \lambda_{ex1} \eta_B}$$

φ : quantum yield; I : integrated area under the uncorrected emission spectra; A : absorbance at the excitation wavelength; λ_{ex} : the excitation wavelength; η : the refractive index of the solution.

(b) Two-photon absorption cross-section

The two-photon absorption (TPA) cross-section (δ) is an important parameter for a two-photon fluorescence probe. Using fluorescein as the reference, the fluorescence intensity of PX-1 (10 μM, pH = 8.2, 10 mM PBS) was measured by two-photon excitation at 800 nm after reaction with $ONOO^-$ (10 μM) by using fluorescein (3.25×10^{-7} M) as the reference. The TPA cross-section of PX-OH was determined to be 24.3 GM according to a standard equation (2).

$$\delta_s = \delta_r \frac{\varphi_r C_r n_r F_s}{\varphi_s C_s n_s F_r}$$

The subscripts s and r refer to the sample and the reference material, respectively. δ: TPA cross-sectional value; C: the concentration of the solution; n: refractive index of the solution; F: TP excited fluorescence integral intensity; φ: the fluorescence quantum yield. PX-1 emitted at approximately 562 nm and was excited at 800 nm (TP).

Synthesis of probe PX-1

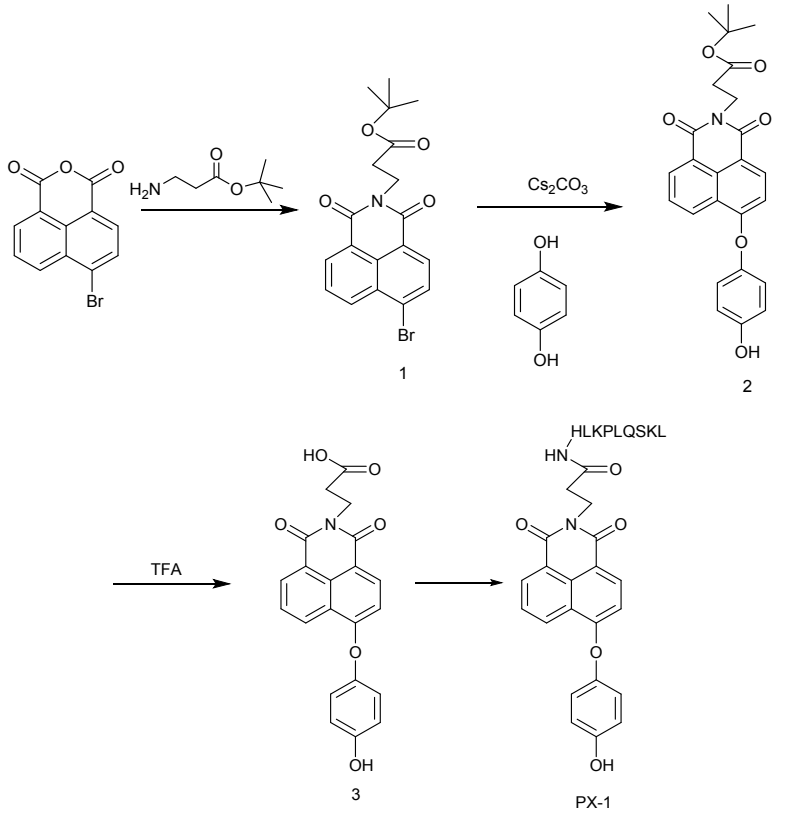

Scheme S1 Synthesis of PX-1.

This new peroxisomal-targeting fluorescent probe PX-1 was synthesized according to the above steps. Compound 1 was prepared according to the literature.[1] The synthesis of compound 2 and 3 were described below.

The mixture of compounds 2 (1.0 mmol, 0.277 g) and 1, 4-dihydroxybenzene (3.0 mmol, 0.330 g) in 15 ml of anhydrous acetonitrile followed by Cs_2CO_3 (3.0 mmol, 0.978 g). Then, the reaction solution was stirred at 90 °C overnight. After that, the mixture was subjected to suction filtration to remove the residual Cs_2CO_3. The solvent in the collected filtrate was evaporated, and the product was purified by silica gel column chromatography (CH_2Cl_2/MeOH = 10: 1, v/v) to give the pure compound 2 (0.073, 16 %), pale yellow solid. ^{1}H NMR (d_6-DMSO, 400 MHz): δ 1.32 (s, 9H), 2.56 (t, J = 7.2 Hz, 2H), 4.23 (t, J = 7.2 Hz, 2H), 6.86 (d, J = 8.4 Hz, 1H), 6.91 (d, J = 9.2 Hz, 2H), 7.13 (d, J = 8.8 Hz, 2H), 7.89 (m, 1H), 8.36 (dd, J_1 = 8.4 Hz, J_2 = 3.6 Hz, 1H), 8.53 (d, J = 6.8 Hz, 1H), 8.70 (d, J = 8.4 Hz, 1H), 9.68 (s, 1H). ^{13}C NMR (d_6-DMSO, 100 MHz) δ 28.09, 33.97, 36.17, 80.60, 110.04, 115.77, 117.21, 122.27, 122.68, 123.37, 127.43, 128.90, 129.40, 131.97, 133.50, 146.37, 155.79, 160.83, 163.22, 163.92, 170.66. HRMS (ESI): calculated for $C_{25}H_{23}NO_6$, $[M+Na]^+$ = 456.1325, found 456.1406.

Compound 3 (1.0 mmol, 0.457 g) was dissolved in 2.0 ml of anhydrous CH_2Cl_2, and then 4.0 ml of CH_2Cl_2/CF_3COOH (1: 1, v/v) were added and stirred at room temperature for 4 h. The solvent was removed, and the resulting crude product was purified by column chromatography (CH_2Cl_2/MeOH = 8:1, v/v) to give pure compound 3 (0.366 g, 80 %), pale yellow solid. ^{1}H NMR (d_6-DMSO, 400 MHz) δ 2.55 (t, J = 7.6 Hz, 2H), 4.23 (t, J = 7.6 Hz, 2H), 6.86 (d, J = 8.4 Hz, 1H), 6.93 (d, J = 8.8 Hz, 2H), 7.11 (d, J = 8.8 Hz, 2H), 7.88 (t, J = 7.8 Hz, 1H), 8.36 (d, J = 8.4 Hz, 1H), 8.53 (d, J = 7.2 Hz, 1H), 8.70 (d, J = 8.0 Hz, 1H). ^{13}C NMR (d_6-DMSO, 100 MHz) δ 33.73, 36.71, 110.03, 115.85, 117.26, 122.55, 123.38, 127.39, 128.81, 129.40, 131.91, 133.43, 148. 29, 155.96, 160.80, 183.22, 133.92, 173.62. HRMS (ESI): calculated for $C_{21}H_{15}NO_6$, $[M-H]^-$ = 376.0819, found 376.0815.

PX-1 was provided by Sangon Biotech.

The final structures of compound 2 and 3 were well-characterized with ^{1}HNMR, ^{13}C NMR, and high-resolution mass spectrometry (HRMS). PX-1 was well-characterized with HRMS and HPLC.

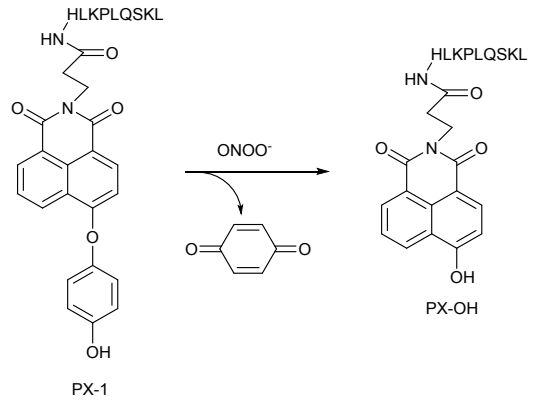

Scheme S2 The sensing mechanism PX-1 with $ONOO^-$. Two mass peaks were observed at m/z = 1330.27 and m/z = 108.02 in the reaction solution, corresponding to PX-OH ($[M + 2H]^{2+}$ = 666.14) and the byproduct p-benzoquinone ($[M + Na]^+$ = 131.00), respectively.

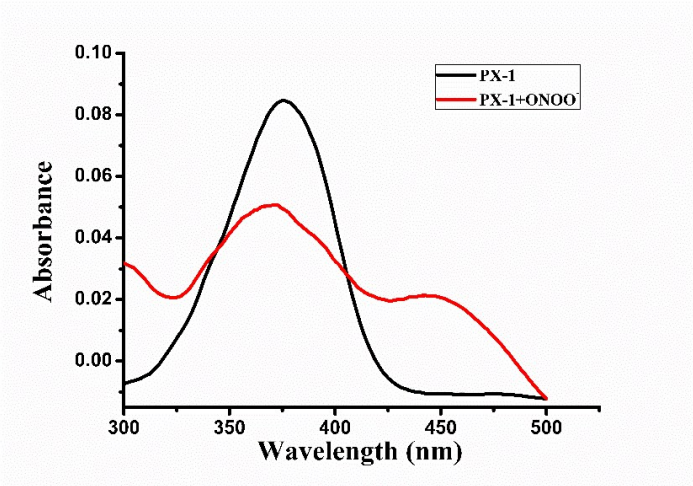

Fig. S1 Absorption spectra of PX-1 (10.0 μM) in the absence or presence $ONOO^-$ (10.0 μM, 30 min).

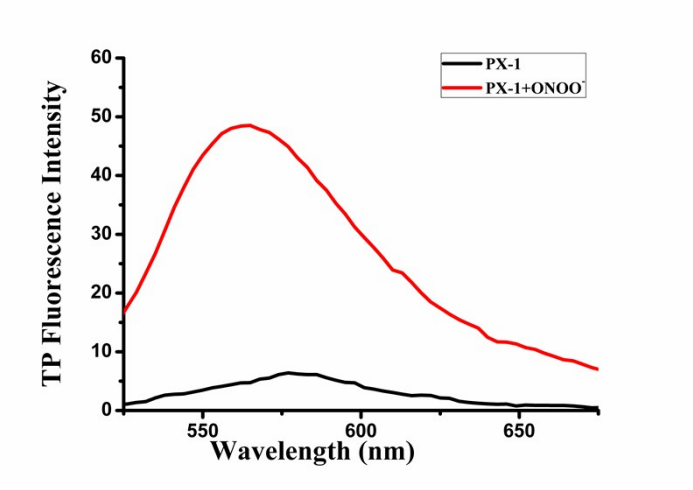

Fig. S2 Two-photon fluorescence spectra of PX-1 (10.0 μM) before and after adding the $ONOO^-$ (25.0 μM, 30 min). λ_{ex} = 800 nm.

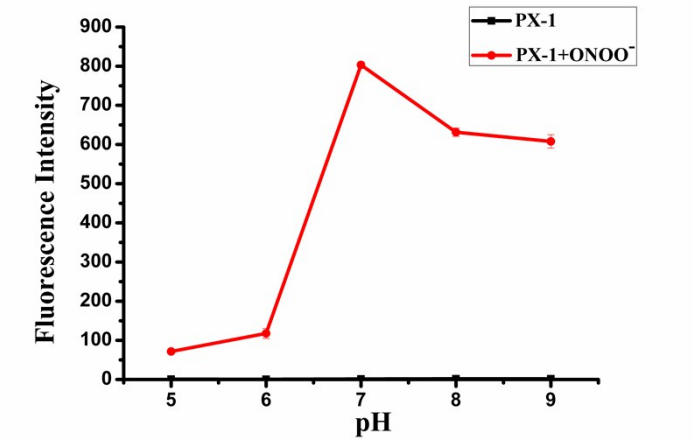

Fig. S3 The fluorescence intensity of PX-1 (10.0 μM) at 553 nm to $ONOO^-$ (25.0 μM, 30 min) under different pH values (5.0-9.0). λ_{ex} = 405 nm, λ_{em} = 553 nm. As aboved data, PX-1 responded well with ONOO- under neutral and weak alkaline conditions.

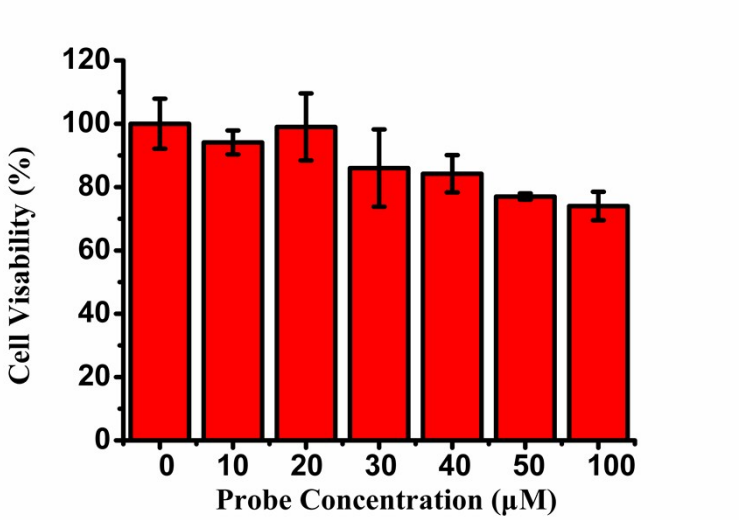

Fig. S4 MTT assay of HL-7702 cells in different concentrations of PX-1.

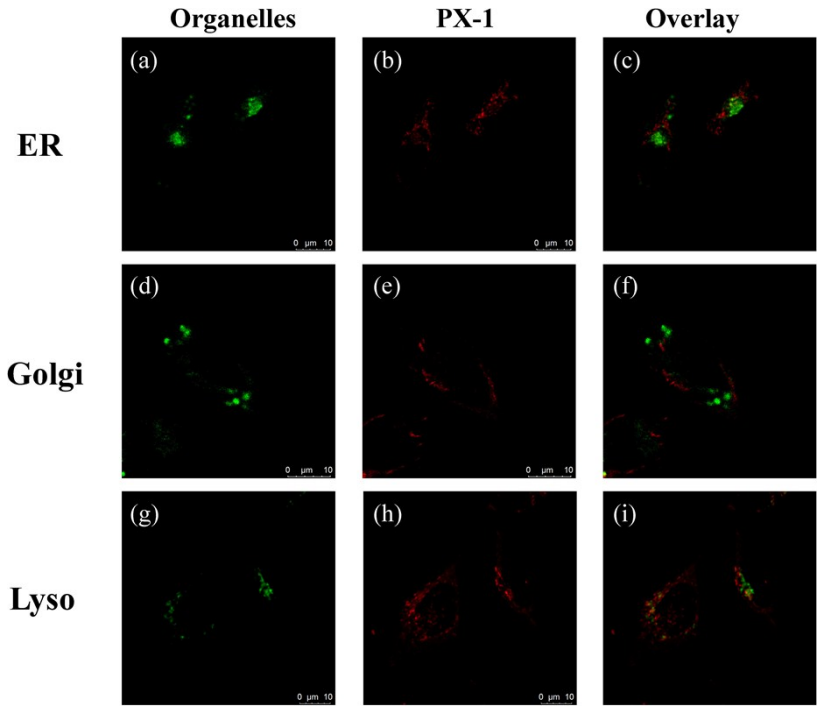

Fig. S5 Co-localization fluorescence images of SMMC-7721 cells stained with PX-1 and other organelles after being induced with SIN-1. First, SMMC-7721 cells were stained with SIN-1 (1.0 mM, 30 min), then treated with PX-1 (5.0 μM) and organelle dyes for 30 min, including Golgi-Track Red (50 nM, λ_{ex} = 561 nm, λ_{em} = 580–630 nm), ER-Tracker Red (50 nM, λ_{ex} = 561 nm, λ_{em} = 580–630 nm), Lyso-Tracker Deep Red (100 nM, λ_{ex} = 633 nm, λ_{em} = 650–750 nm). The co-localization coefficient was about 0.09, 0.31 and 0.40 for endoplasmic reticulum, Golgi apparatus and lysosomes, respectively. So, PX-1 exhibited the poor co-localization with other organelles. Scale bar: 10 μm.

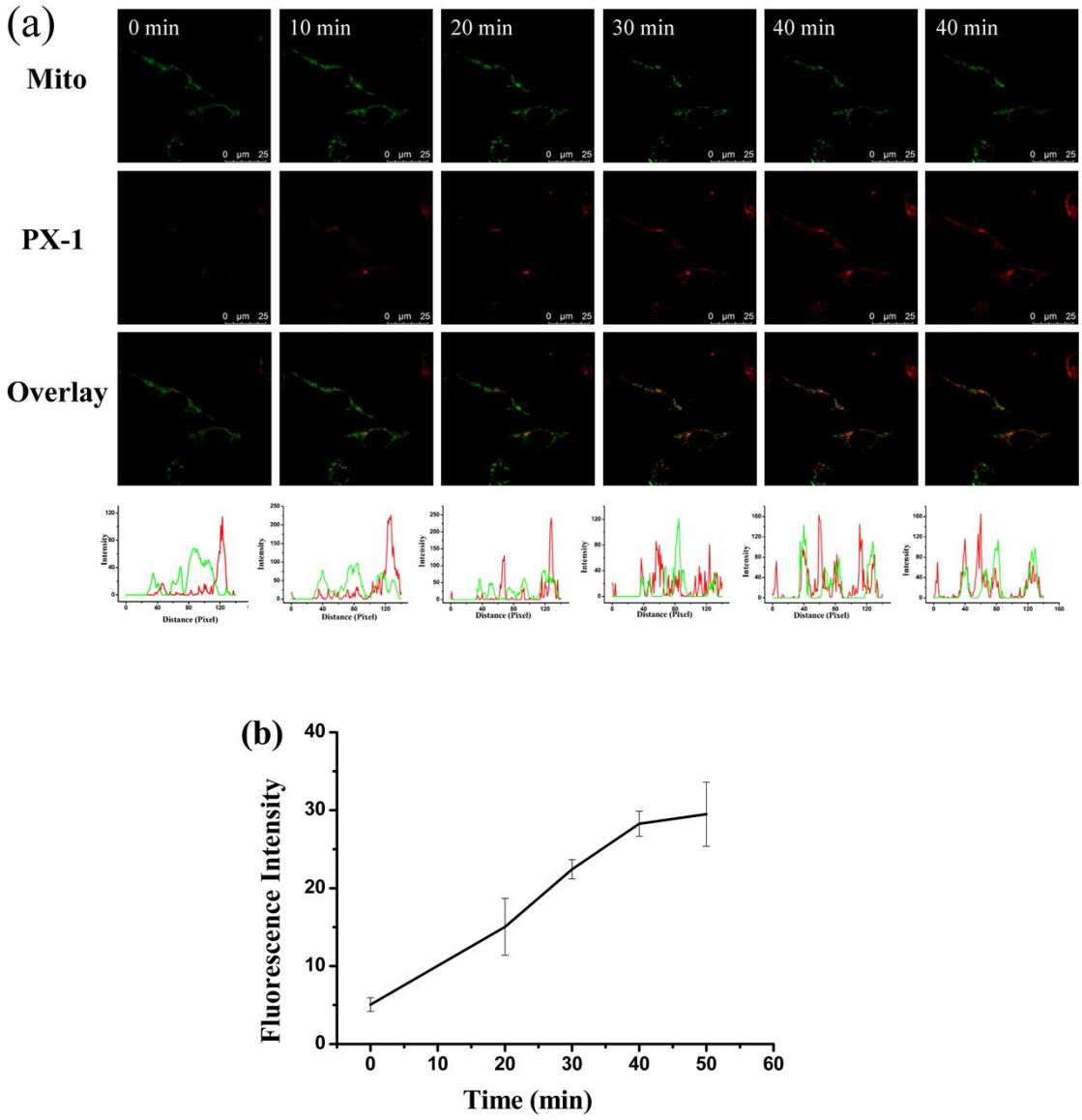

Fig.S6 (a) The time-dependent fluorescence imaging of SMMC-7721 cells incubated with PX-1 and Mito-Tracker Deep Red. (b) The output of normalized average fluorescence intensity of PX-1 with increase of time (0-50.0 min). The fluorescence images of SMMC-7721 cells incubated with SIN-1 (1.0 mM) for 30 min, then treated with PX-1 (5.0 μM) and Mito-Tracker Deep Red (100 nM) for 15 min. The co-localization coefficient was about 0.26, 0.43, 0.22, 0.30, 0.34 and 0.35 with the increase of time. PX-1, λ_{ex} = 405 nm, λ_{em} = 536-650 nm, Mito-Tracker Deep Red, λ_{ex} = 633 nm, λ_{em} = 650–750 nm. Scale bar: 25 μm.

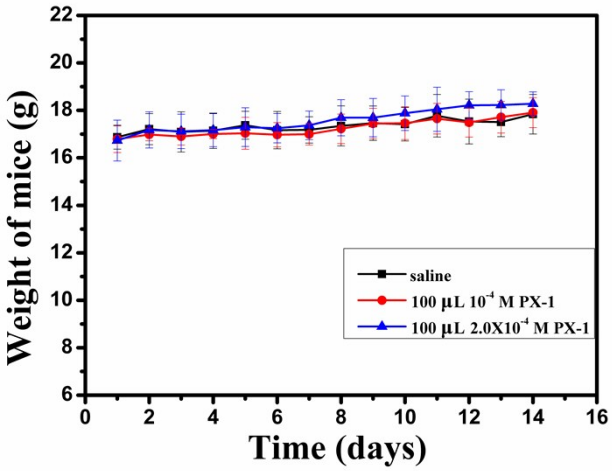

Fig. S7 *In vivo* toxicity of PX-1 in C57 mice. C57 mice were randomly divided into three groups, control group, experimental group. Experimental group were treated with different PX-1 (100 µL, 10^{-4} M and 2.0×10^{-4} M) by intragastric administration. The control group were treated with 100 µL saline. The weight changes of mice in the experimental group were compared with control group for two weeks. The results showed that the body weight of mice in the experimental group were basically as the same as that of the control group. Moreover, the mice in the experimental group didn't show any disease symptoms such as hair loss, scarring and vomiting. Therefore, PX-1 exhibits low cytotoxicity *in vivo*. 5 mice in each group.

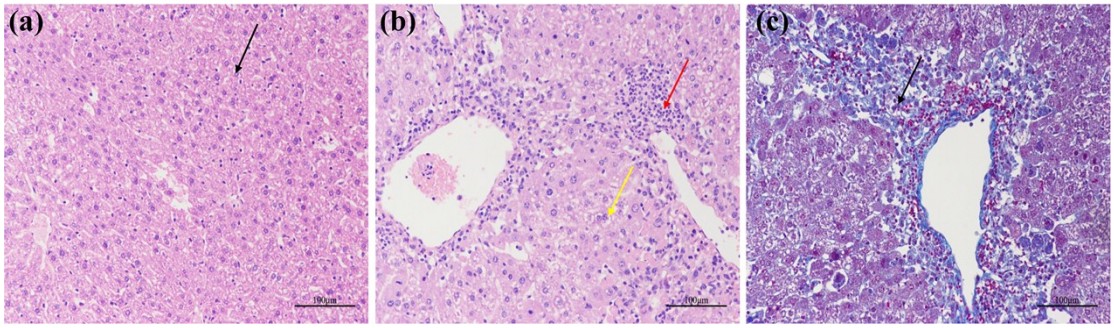

Fig. S8 The hematoxylin and eosin (H&E) staining of liver in mice. (a) Normal liver tissue. The morphology of hepatocytes is not obvious inflammatory cell infiltration (black arrow). (b) and (c) Liver tissue of mice caused by CCl_4. Necrosis, pyknosis and dissolution of hepatocytes (black arrow), extensive inflammatory cell infiltration and marked fibrosis (red arrow), accompanied by varying degrees of swelling, vacuolar degeneration around necrotic hepatocytes (Yellow arrow). Scale bar = 100 µm.

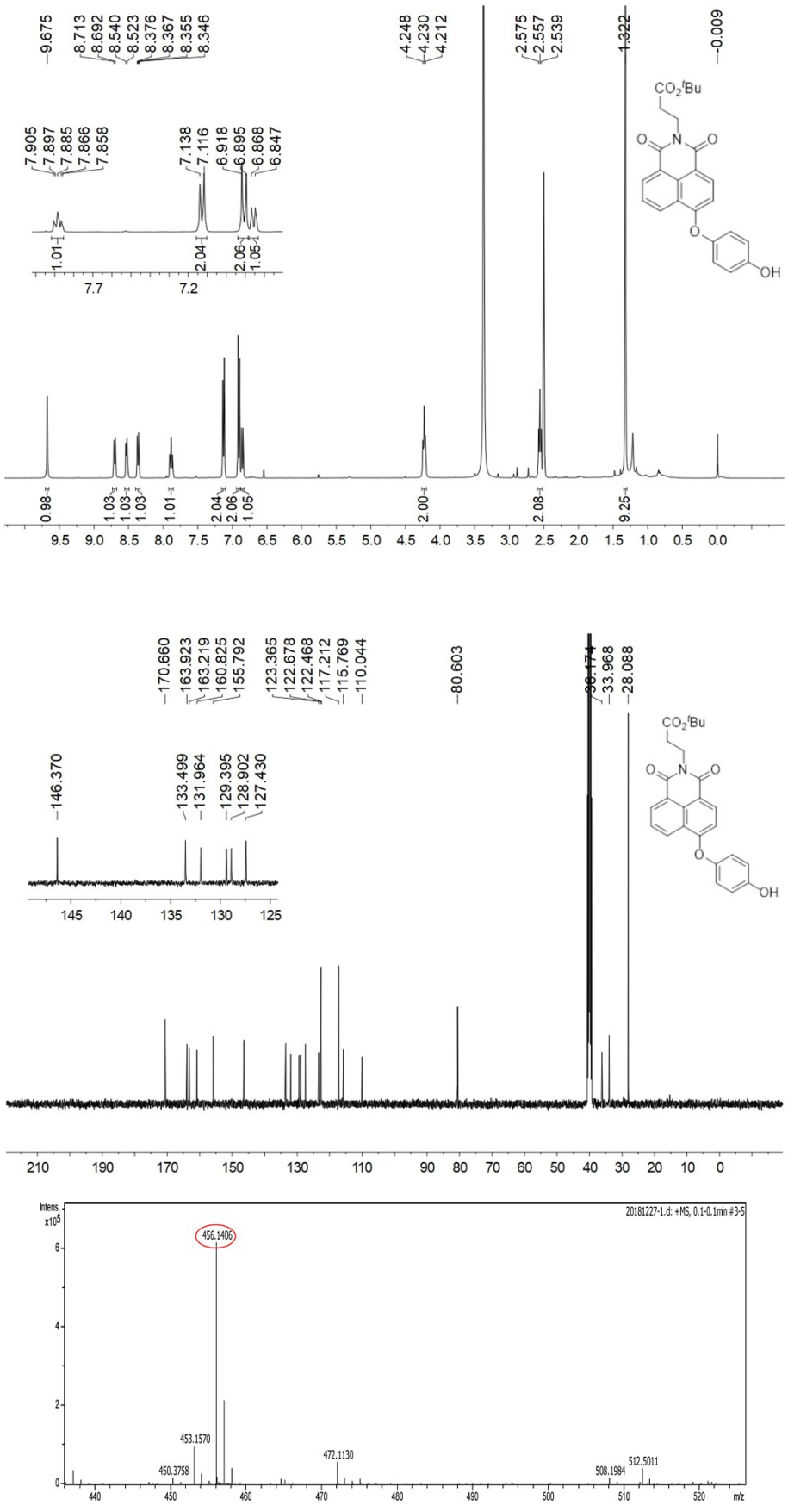

Fig. S9 The ^{1}H NMR, ^{13}C NMR and HRMS data of compound 2.

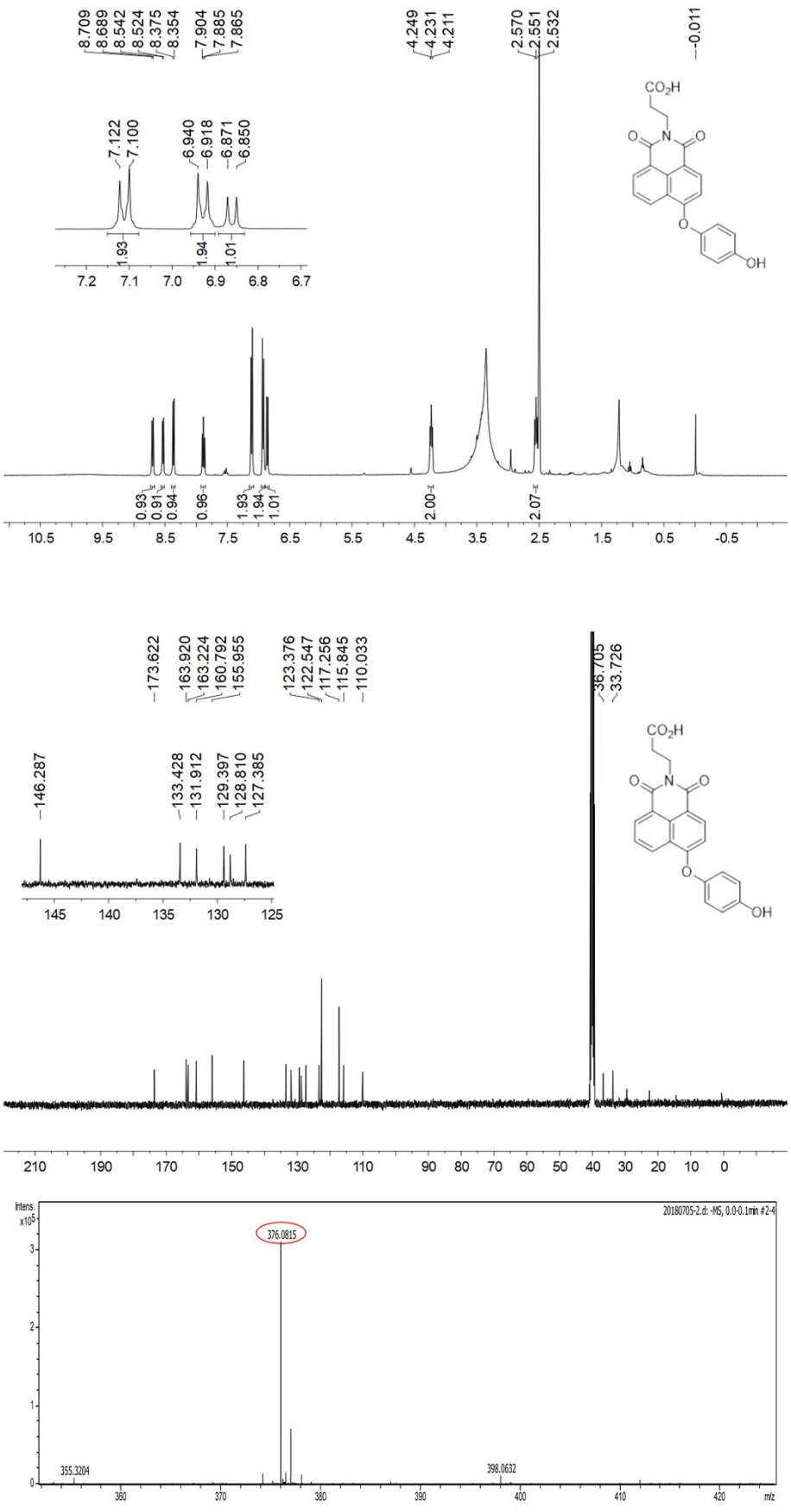

Fig. S10 The ^{1}H NMR, ^{13}C NMR and HRMS data of compound 3.

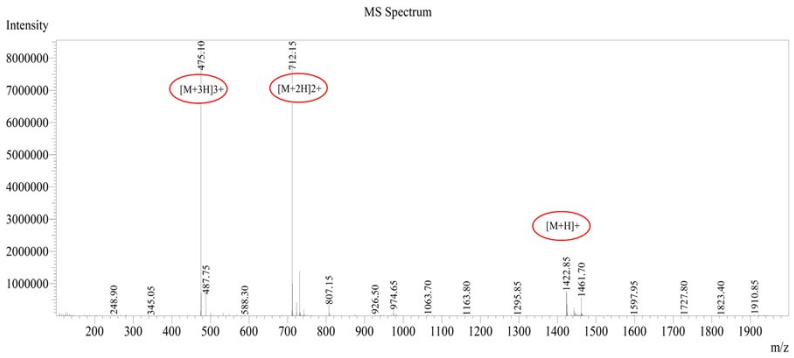

Sample Information

Name	:	PX-1
Sequence	:	1-HLKPLQSKL
Modification	:	N/A
Pump A	:	0.1%trifluoroacetic in 100%water
Pump B	:	0.1%trifluoroacetic in 100%acetonrtrile
Total Flow	:	1.0ml/min
Wavelength	:	214nm
Analytical column type	:	SHIMADZU Inertsil ODS-SP(4.6*250MM*5UM)
Dissolution method	:	0.1mg sample dissolved to 0.5mL by 100%H2O
Acquisition Time	:	2018/08/09 10:36:12
Inj.Volume	:	70ul

Time	Module	Action	Value
0.01	Pumps	B.Conc	26
20.00	Pumps	B.Conc	46
20.01	Pumps	B.Conc	95
27.01	Pumps	B.Conc	95
27.02	Controller	Stop	

Chromatogram

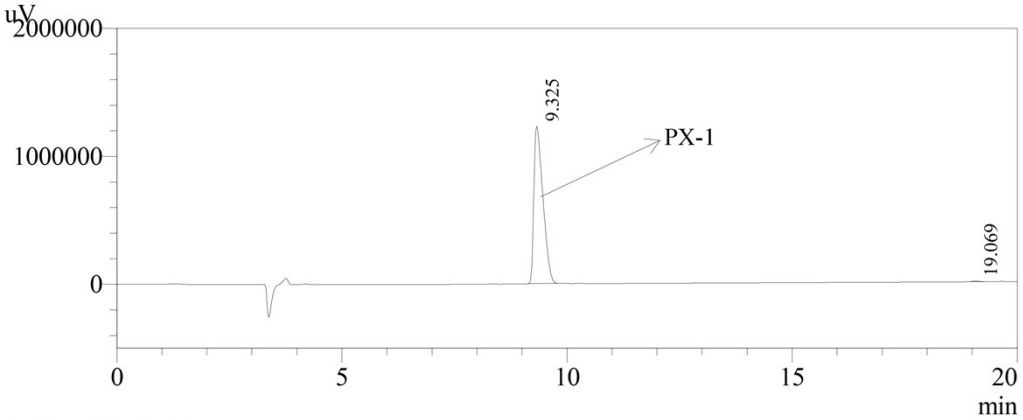

1 Det.A Ch1 / 214nm

PeakTable

Detector A Ch1 214nm

Peak#	Ret. Time	Area	Height	Area %	Height %
1	9.325	17123279	1227702	99.781	99.673
2	19.069	37510	4032	0.219	0.327
Total		17160789	1231734	100.000	100.000

Fig. S11 The MS and HPLC data of probe PX-1.

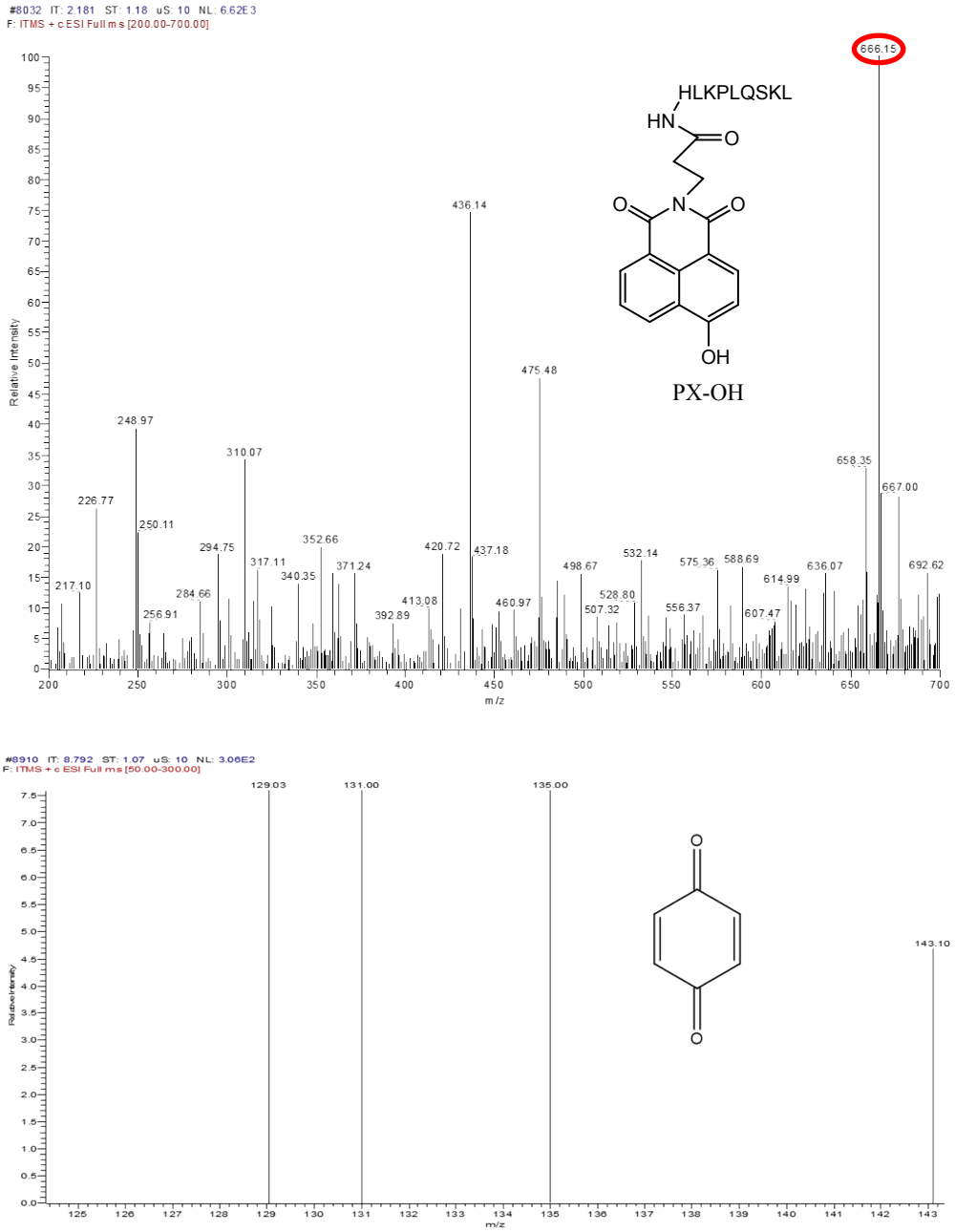

Fig. S12 The MS data of compound the PX-OH and by-product.

References

(1) Y. Li, X. L. Xie, X. E. Yang, M. M. Li, X. Y. Jiao, Y. H. Sun, X. Wang, B. Tang, *Chem. Sci.*, 2017, **8**, 4006.